Axial Behavior of Innovative Sand-Coated GFRP Piles in Cohesionless Soil

Ahmad Almallah, Hany El Naggar[1], and Pedram Sadeghian

Department of Civil and Resource Engineering, Dalhousie University, 1360 Barrington St., Halifax, NS, B3H 4R2, Canada

Abstract

In pile construction, conventional pile materials such as concrete, steel, and wood are frequently subject to soil-substructure interaction durability problems due to corrosion and deterioration. Fiber-reinforced polymers (FRP) provide a potential alternative to eliminate the durability problems of conventional materials. This paper describes the results of an experimental study on the effect of the interface on the behaviour of glass FRP (GFRP) piles jacked into dense sand under axial loads. The aim of this study is to introduce an innovative GFRP piles in cohesionless soil through coating its surface with silica sand to enhance the pile interface behaviour. The experimental program investigates seven small-scale GFRP piles with different surface roughness and a reference steel pile, used as a control. The surface of five of the seven GFRP piles was coated with silica sand, and the performance of the GFRP piles was compared with that of the control steel pile. The results of the pile load tests were analyzed by using three different commonly used methods to determine the ultimate pile load capacities. The results showed that the innovative mechanism of coating GFRP piles with silica sand enhanced the interface friction of the GFRP piles in sand under axial loads and increased the ultimate pile load capacity in comparison with that of the control piles.

DOI: https://doi.org/10.1061/(ASCE)GM.1943-5622.0001808

[1] Corresponding Author: hany.elnaggar@dal.ca

Keywords: Pile**,** Glass fiber-reinforced polymers, Sand coating, Interface friction, Pile capacity.

INTRODUCTION

Pile foundations are generally used to transfer structural loads to the soil when shallow foundations are insufficient to carry the loads, or when soil suitable for construction is located deep beneath the ground surface. Based on the mechanism of transferring loads from the structure to the soil, there are two types of piles, as described in AASHTO (2002): An end bearing pile transfers loads via the end toe, whereas a friction pile transfers loads via skin friction. Conventional materials such as concrete, steel, and wood have long been used to manufacture piles. However, in comparison to alternative materials, these conventional materials are more likely to be subject to soil interface problems due to corrosion and deterioration of the materials when they are used in harsh environments or offshore construction. In the past few years, fiber-reinforced polymer (FRP) composites have been used increasingly in pile design to overcome pile-soil interface problems (Guades et al. 2010). FRP composites are lighter, stronger, and have lower maintenance costs than conventional pile materials as they are more corrosion resistant, this makes them cost-effective for use in construction (Zobel et al. 2005). Glass FRP (GFRP) composites are among the most cost-effective composites and have the advantage of durability in harsh environments. In 1998, Iskander and Hassan used GFRP composites for marine fendering and light bearing applications. Frost and Han (1999) studied the interface friction behaviour of FRP in sand. The results showed that the interface friction between FRP and sand depends upon the FRP surface roughness, the normal stress, and the sand particle angularity. Pando et al. (2000) conducted a full-scale pile load test by comparing FRP tubes filled with concrete and precast concrete piles. It was found that the two types of the pile have a similar axial capacity in compression. Toufigh et al. (2013) found that

carbon FRP (CFRP) can be beneficial as reinforcement in earth structures, due to its high friction angle with soil and high tensile strength.

Investigating the effect of FRP surface roughness on the shear stress along a pile shaft in cohesionless soils is necessary to adopt these new composites in the pile foundation industry. In 2005, Sakr et al. studied the interface characteristics and constructability of FRP piles filled with concrete in comparison to a steel reference pile. The findings indicated that the interface friction angle of an FRP pile in dense sand is similar to or greater than that of a reference steel pile. Abuel-Naga and Shaia (2014) studied the changes in surface topography and interface friction of FRP plates sheared against different types of sand. The results showed that the peak interface shear coefficient between the plate material and the soil decreases as the normal soil stress increases. Toufigh et al. (2015) and Toufigh et al. (2016) determined that the surface roughness of FRP, and polymer concrete (PC) is the controlling parameter for the interface friction between the tested material and soil. Vineetha and Ganesan (2014) conducted direct shear tests to investigate the interface friction between GFRP and gravel. They found that the interface friction angle was greater when the fiber direction was perpendicular to the shearing load.

The drivability of FRP composites in soil is a concern for pile construction due to its drivability limitations (Ashford and Jakrapiyanun, 2001). Guades et al. (2012) evaluated the performance of driven hollow FRP piles. They found that the factors affecting the driving of FRP piles are the type of driving hammer used, the resistance of surrounding soil, the pile axial stiffness, and the strength of the pile material. Spiro and Pais (2002) performed driving tests and found that the FRP pile driving capacity was 27% higher (harder to drive) than that of a prestressed concrete pile. El Sharnouby and El Naggar (2018) indicated that calibration may be required for FRP-micro piles under compression due to its installation method.

The reason GFRP piles were chosen in this research was due to its sustainable characteristics, including the capability of having a longer service life than the conventional piling materials without the need for rehabilitation or significant maintenance. In addition, enhancing the interface friction between GFRP piles and soil can increase the capacity of the GFRP piles. Also, the proposed coating technique of bonding sand to the GFRP pile using an epoxy resin during the manufacturing of the pile provides more compatibility with the base material and more feasible from the manufacturing point of view.

Direct shear tests are an effective method of obtaining the strength parameters of the soil-structure interface. To investigate the interface friction between GFRP and sandy soils, Almallah et al. (2018) conducted several direct shear tests on GFRP specimens with different surface roughness in sandy soils and found that the GFRP surface roughness was the controlling parameter for interface friction. Almallah et al. (2019) introduced a mechanism for enhancing GFRP surface roughness by coating the surface of several GFRP specimens with silica sand. Sand-coated GFRP specimens with different coating densities (0, 500, 1000, 1500, 2000, and 2500 g/m^2) were tested by using interface shear tests. It was shown that coating the surface of GFRP specimens with silica sand with coating density of 1500 g/m^2 yielded optimal results for increasing the angle of interface friction of GFRP specimens in poorly graded sand, while GFRP specimens with sand coating density of 2000 g/m^2 yielded optimal results in silty sand and sandy lean clay.

However, direct shear test results alone are not sufficient to understand and confirm the interface friction behaviour of GFRP piles in sand. Moreover, GFRP composites have not yet gained wide acceptance in foundation design and geotechnical practice due to a lack of research and design guidelines. The present study was therefore designed to enhance the interface friction behaviour of GFRP piles driven by jacking into dense sand by introducing an innovative

mechanism for coating the pile surface with silica sand, using different sand coating densities to provide a roughened skin for friction piles.

MATERIALS AND METHODS

GFRP piles coated with sand with different coating densities were driven into sand and then tested under axial loads. The following sections present details of the experimental program.

Test Matrix

A total of seven GFRP piles 760 mm in length (L) with outer diameters (D) ranging from 50 mm to 61 mm (depending upon the density of the sand coating) were prepared. Each GFRP pile was fabricated from four layers of unidirectional fiberglass fabric and epoxy resin. Silica sand was added to the surface of five of the seven GFRP piles. The test parameter was the density of the GFRP pile sand coating. The GFRP piles were roughened via coating its surface with silica sand. The magnitude of roughness was controlled through different densities of sand coating (g/m^2). The silica sand particles were weighed in grams (g) based on the desired sand coating ratio and then sparkled over the GFRP pile surface area, which is in m^2. The uniformity of sand coating over the GFRP sheets area was controlled manually by ensuring a uniform distribution of the sparkled sand over the surface area and uniform distance between the sand coating particles. The sand coating densities examined in this study were 500, 1000, 1500, 2000, and 2500 g/m^2. Two of the GFRP piles were not coated in sand; instead, the surface of one of the piles was roughened, and the surface of the other pile was smoothed. A control steel pile was used for purposes of comparison with the GFRP piles. The specimen identification (ID) symbols used for the test piles in Table 1 are Steel and GFRP-*X*, where Steel refers to a steel pile, GFRP indicates a GFRP pile, and *X*

denotes the surface treatment or coating density of a GFRP pile. For example, GFRP-1500 refers to a sand-coated GFRP pile with a sand coating density of 1500 g/m^2.

Material Properties

GFRP

All GFRP piles were prepared with four layers of unidirectional fiberglass fabric. Each GFRP composite pile weighed approximately 3440 g/m^2 without sand coating. Each pile was bonded by an epoxy resin (West System 105) chosen for its superior characteristics (Soltannia and Sameoto, 2014) and a hardener (West System 206). The fiberglass fabric (dry fiber) had a tensile strength of 1500 MPa, a real fabric weight of 450 g/m^2, an elongation of 2.8%, and an elastic modulus of 72 GPa, according to specifications provided by the manufacturer (Haining Anjie Composite Material Co., Zhejiang, China). The elastic modulus and tensile strength of the GFRP composite were determined to be 32 GPa and 502 MPa, respectively, based on tensile tests of GFRP composite specimens.

Coating Sand

Sieve analysis testing was carried out in accordance with ASTM C136-14 (2014) to determine the properties of the silica sand used for coating the GFRP composite piles. As indicated by the silica sand gradation curve plotted in Figure 1(a), the D_{10}, D_{30}, D_{50}, and D_{60} values were 1.1, 1.4, 1.8, and 1.9, respectively. The coefficient of gradation (C_c) was found to be 0.9, and the uniformity coefficient (C_u) was 1.7. The percentage of the total silica sand sample retained on sieve #16 was 96.3%, based on the sieve analysis test. In general, the silica sand used was classified as poorly graded sand (SP), in accordance with the Unified Soil Classification System (USCS). Only silica sand retained on sieves #16 and #8 was used for coating the surface of the GFRP piles.

Soil

The soil used for this experimental study was masonry sand. Sieve analysis testing in accordance with ASTM C136-14 (2014) was used to classify the engineering properties of the masonry sand. As indicated by the gradation curve for poorly graded sand (SP) plotted in Figure 1(a), the D_{10}, D_{30}, D_{50}, and D_{60} values were 0.2, 0.3, 0.5, and 0.6, respectively. The coefficient of gradation (C_c) was found to be 0.9, and the uniformity coefficient (C_u) was 3.0. Soil laboratory compaction characteristics using standard effort were examined in accordance with ASTM D698-12 (2012) to determine the maximum dry density of the masonry sand used and the optimum water content, as shown in Figure 1(b). The maximum dry density of the poorly graded masonry sand was 1746 kg/m^3, and the optimum water content was 14.5%.

Steel

The steel used in this study had a yield tensile strength of 215 MPa, and a modulus of elasticity (*E*) of 195 GPa, based on ASTM A269/A269M.

Aluminium

The aluminium cone used in this study as a shoe for the piles had a yield tensile strength of 240 MPa, and a modulus of elasticity (*E*) of 69 GPa.

Specimen Fabrication

A total of seven GFRP piles were fabricated, each with an initial length of 820 mm and a target outer diameter (D) of 54 mm. Each pile consisted of four layers of glass fabric bonded together with epoxy resin and hardener. The glass fiber layers of each GFRP composite pile were fabricated with fiber directions arranged in the order: [90/0/0/90]. The 0-degree layers (each measuring 820 mm x 160 mm) were axial with no overlap, while the 90-degree layers (each measuring 820 x 210 mm) were hoop layers with 50 mm overlap.

As shown in Figure 2, a plastic pipe with a length of 1840 mm and an outer diameter of 45 mm was wrapped with a plastic sheet 900 mm long. The surface of the plastic sheet was then brushed gently with epoxy resin and hardener. The first layer of fiberglass (a 90-degree hoop) was wrapped tightly around the plastic pipe. During the wrapping process, 68.23 g of epoxy resin and hardener were applied to the glass fiber layer. The other three glass fiber layers were wrapped similarly, with the same amount of epoxy resin and hardener added for each layer. After wrapping of the GFRP four layers was completed [90/0/0/90], the individual piles were covered with wax paper for curing. During the first 30 minutes of the curing process, each pile was rotated frequently by turning the long plastic pipe resting on wooden blocks at both ends, to ensure that the resin was distributed evenly. All specimens were cured at room temperature for a total of seven days after fabrication. When curing was completed, a blade saw was used to remove 50 mm from both ends of each pile, to obtain a pile with a length of 720 mm without the pile tip and an outer diameter of approximately 54 mm.

The surface of five of the seven GFRP piles was coated in silica sand, using five different sand coating densities: 500, 1000, 1500, 2000, and 2500 g/m^2. Following surface treatment, the weight per unit surface area of the GFRP-Smooth, GFRP-Rough, GFRP-500, GFRP-1000, GFRP-1500, GFRP-2000, and GFRP-2500 composite piles was 3438.5, 3546.2, 3864.7, 4134.4, 4820.6, 5585.2, and 6723.1 g/m^2, respectively. The sand was applied uniformly to the surface of each pile after adding epoxy resin and hardener to the pile surface. During fabrication, the GFRP-Smooth pile was tightly wrapped and covered with wax paper to obtain a smooth surface, whereas the surface of GFRP-Rough pile was not covered with wax paper and was left to cure at room temperature. Figure 3 shows the GFRP piles with different sand coating densities used in this

study. A steel pile was prepared as a control specimen to be compared with the GFRP piles. An aluminium cone 40 mm in length was added to the tip of each of the eight piles.

Test Setup and Instrumentation

A small-scale steel frame with a soil tank, illustrated in Figures 4 and 5, was developed at Dalhousie University to test eight small-scale piles with a length (L) of 760 mm with pile cone tip, an outer diameter (D) ranging from 50 to 61 mm, and a L/D ratio ranging from 12.5 to 15.2, as shown in Table 1. The boundary conditions of this experiment at the toe in the vertical and lateral directions satisfy the boundary conditions according to Vipulanandan et al. (1989), and Sakr et al. (2004) to ensure that the boundary effects are not interfering with the tested pile. Each pile used in this study was tested with a pile head 150 mm in diameter at the top of the pile, and a cone-shaped pile toe with a 45° inside slope and a length of 40 mm. The piles were prepared and jacked-driven into a soil tank measuring 1200 mm x 910 mm. The soil used was poorly graded sand, which filled the soil tank to a depth of 1000 mm. The sand was placed in the tank for each test in 5 layers (each layer approx. 250 mm). Each layer of sand was compacted with a manual tamper. The relative density of the sand in the tank was measured before each pile test via 3 sand cone tests (at the pile tip level, center of pile level, and soil surface) then the average of the three tests was taken into consideration to get the relative density of sand. A hydraulic jack with a maximum stroke of 160 mm was used. A load cell was connected to the end of the jack to measure the load in newtons (N). Two string potentiometers, each with the capability of measuring 609.6 mm, were placed at the top of the hydraulic jack to measure the vertical displacement during the driving of the piles. The load cell and string potentiometers were connected to a data acquisition system (DAQ) to export the test results and display them on a digital screen. To drive each pile, four extension pipes made of aluminium were used, with an outer diameter of 50 mm and lengths of

130, 280, 430, and 580 mm. Each pile was instrumented with two strain gauges near the pile toe, to determine how much load was mobilized through the bearing tip, and along the pile shaft. The average of the strain measured from each of the two strain gauges was determined. Then, the strain measurement was converted to force by multiplying it with the elastic modulus of GFRP, then multiplying it by the pile cross-sectional area. This force was used to get the bearing component, while the friction component was the deduction of the bearing component from the total load. Figures 4, 5, and 6 show the instruments and test setup used in this study.

Test Procedure

As illustrated in Figure 4, eight piles were driven and tested under axial compression loading in accordance with ASTM D1143 (2007). Each pile was jacked into the sand in five stages by using the hydraulic jack, which is essentially free from noise and vibration (Yang et al. 2006), until the distance between the pile head and the surface of the sand in the soil tank was 50 mm, as shown in Figure 5. At each stage, the pile was jacked-driven approximately 160 mm (the maximum stroke of the hydraulic jack) vertically down into the sand, except for the final stage of about 70 mm (depending upon the initial vertical displacement of the pile during the first driving stage). For all stages, the driving rate was 22.7 mm/min.

The first driving stage, performed without using any of the aluminum extensions, began with the pile toe touching the surface of the sand. The pile was driven approximately 160 mm into the sand (depending upon the vertical adjustment of the pile before driving). Then the stroke was retracted into the hydraulic jack, and an aluminum extension 130 mm long was placed between the pile head and the load cell. In the second stage, the pile was driven another 160 mm into the sand. The first extension was then removed while the stroke was again retracted into the hydraulic jack. The third driving stage was performed by using an aluminum extension 280 mm long to drive

the pile a further 160 mm into the sand. The same procedure was repeated for the fourth driving stage, with an aluminum extension pipe 430 mm long. In the final stage, an extension pipe 580 mm long was used, and the pile was jacked a further 70 mm into the sand, so that a distance of 50 mm remained between the pile head and the surface of the sand. Laser light was used to ensure the verticality of the jacked piles during installation.

During each jacking stage, the loading was measured, and the vertical displacement was correlated with the load applied, to plot the load versus displacement curve for each pile. After jacking was completed, a static axial compression load test was performed on the pile head. The static axial load test was performed directly on the pile after the jack-driving within few minutes to prepare the hydraulic jack. The pile load test was carried out to check the pile head settlement of 10% of the 50-mm pile diameter (a settlement of 5 mm), as suggested by De Nicola and Randolph (1999), and the ultimate pile capacity under axial loads. The pile load test was performed to achieve over 22 mm settlement of the pile head, and then the test was stopped. The pile load test was performed with a loading rate of 0.5 mm/min. After completion of the test, the load versus settlement curve was plotted with the values of the ultimate load, friction load, and bearing capacity for each pile. Three different methods of analysis were used for purposes of comparison.

RESULTS AND DISCUSSION

Pile Jack-Driving Results

Each of the eight piles used in this study was jacked-driven into dense sand until the distance between the pile head and the soil surface was 50 mm. In Figure 7, Sx refers to pile sand coating ratio, R to rough pile surface, and S to smooth pile surface. Of all the piles tested, the sand-coated GFRP pile S1500 required the highest loading (13.3 kN) to achieve a pile tip advancement of 680

mm. This was due to strong interlocking between the soil particles and the sand-coated pile surface, which contained sufficient voids to enhance the interface mechanism. Similar results were found for the sand-coated GFRP piles S1000 and S2000, which required driving loads of 12.6 kN and 12.3 kN, respectively, to achieve a pile tip advancement of 680 mm.

The load required to drive the sand-coated GFRP pile S2500 a tip advancement of 680 mm into the soil was only 11.3 kN. This is less than that required for piles with a lower sand coating density, because the S2500 pile had fewer surface voids, resulting in less interlocking between the soil particles and the pile surface and consequently less pile skin resistance. For the control rough GFRP pile (GFRP-R) and the steel pile, similar loads were required to drive the piles so that 50 mm remained between the pile head and the soil surface. At higher pile tip displacement values, the driving curve of the steel pile approached that of the rough GFRP pile. To achieve a tip advancement of 680 mm (before reaching the distance of 50 mm between the pile head and the soil surface), the load required by the steel pile was 10.2 kN, which was 1.1 kN higher than that required by the rough GFRP pile (9.1 kN). As observed by Ashford and Jakrapiyanun (2001), the axial stiffness of piles composed of GFRP is lower than that of steel piles. The smooth GFRP pile had a driving performance similar to that of the rough GFRP pile. Since the rough and smooth GFRP piles had similar driving performance, the pile behaviour was dominated by end-bearing resistance during driving, whereas the sand-coated piles had greater shaft resistance due to increased dilation resulting from interface friction. The vertical red-dashed line was just to indicate specific number (load) for each pile at the end of the jack-driving stages for comparison.

Pile Load Test Results

Pile load tests were performed for all eight piles, by applying a static axial load to the pile head to find the ultimate pile capacity (a combination of the bearing capacity and the friction capacity, as

shown in Figure 8). A summary of the results of the load tests for all the piles is presented in Figures 9 and 10, where Sx refers to pile sand coating ratio, R to rough pile surface, and S to smooth pile surface. The smooth GFRP, rough GFRP and steel piles all exhibit slight post-peak reductions in shaft resistance, whereas the sand-coated generally tend to increase throughout loading as shown in Figure 8, and 10. In order to discuss and analyze the experimental results, Brinch and Hansen method (1963) was used to find the ultimate load capacity, the ultimate bearing capacity, and the ultimate friction capacity of each pile. At the end, two other methods were used (modified Chin (1970), and Decourt (1999)) for comparison. The following sections present the discussion of pile load test results.

Brinch Hansen Method (1963)

This method is used to determine the ultimate capacity of a pile (Q_{ult} in kN) from the pile load test total load versus settlement graph (Figure 9), by finding the load on the curve that corresponds to a settlement value two times the settlement of 0.9 Q_{ult}. The ultimate tip bearing capacity and the ultimate friction capacity are taken from the corresponding values of the settlement at Q_{ult}. The values of the ultimate capacities of all the piles according to the Brinch Hansen method (1963) are presented in Table 2 and Figure 11.

As per Brinch Hansen (1963), of the piles tested, the pile with the highest ultimate pile capacity was the sand-coated GFRP pile S1500 (having a sand coating density of 1500 g/m^2), with an ultimate pile capacity of 15.5 kN. This value is 23% higher than the ultimate capacity of the rough control pile GFRP-R, and 31% higher than ultimate capacity of the reference steel pile. The friction component of the S1500 pile, which carried 6.7 kN of the total ultimate load, was 52% and 60% higher than the friction components of the uncoated GFRP-R pile and the control steel pile, respectively. Thus, the newly proposed GFRP pile S1500, coated with 1500 g/m^2 of silica

sand, not only has greater durability than piles made of conventional materials, but also has a high ultimate capacity due to its rough coating and strong interlocking between the pile surface and soil particles.

As shown in Figure 11, the introduced sand coating mechanism enhanced the interface friction and the ultimate capacity of GFRP piles, especially in the case of sand coating densities of 500, 1000, 1500, and 2000 g/m^2. Using a sand coating density greater than 2000 g/m^2 resulted in a lower ultimate GFRP pile capacity, similar to that of the control GFRP pile, because interlocking between the pile surface and soil particles was weaker due to the smaller number of voids in the coated pile surface. This accounts for the lower capacity of sand-coated pile S2500.

Modified Chin Method (1970)

In the modified Chin method, the ultimate capacity of a pile is determined by plotting the curve of the settlement/load on the *y*-axis versus the settlement on the *x*-axis. The value of the ultimate capacity is given by the inverse of the slope of the resulting line multiplied by 1.2. The values of the ultimate bearing capacity and ultimate friction capacity can be identified from the corresponding settlement at the ultimate capacity (Q_{ult}). The values of the ultimate capacities of all the piles according to the modified Chin method (1970) are presented in Table 3.

As in the case of the Brinch Hansen method, according to the modified Chin method (1970), of the piles tested, the pile with the highest ultimate pile capacity was the S1500 pile. The consistent results yielded by the two methods lend support to the effect of coating the surface of GFRP piles with silica sand to enhance the interface friction resistance of this composite material, which could provide an alternative to conventional pile materials when needed. With the modified Chin method, the friction component of the S1500 pile was found to be 52% and 58% higher the friction components of the control GFRP-R and steel piles, respectively.

Decourt Method (1999)

In this study, the third method used to determine the ultimate pile capacity was the Decourt method (1999). This method divides each load on the pile head by the corresponding settlement and plots the resulting value on the *y*-axis against the applied load on the *x*-axis. The ultimate load is identified by the intersection of the linear regression (using the last three points) of the curve with the *x*-axis (applied load). The ultimate bearing load and the ultimate friction load are identified by the corresponding settlement at Q_{ult}. The values of the ultimate capacities of all the piles according to the Decourt method (1999) are presented in Table 4.

As in the case of the Brinch Hansen and modified Chin methods, according to the Decourt method (1999), of all the piles investigated, the S1500 pile had the optimum ultimate capacity. As shown in Table 4, the S1500 pile had the highest friction component and the S1000 pile had the second highest friction component, due to the large settlement at Qult. The results of Figure 13 confirm the findings of Figures 11 and 12 in terms of the effectiveness and significance of the newly proposed sand-coated GFRP S1500 pile. These findings can benefit the pile design and manufacturing industry especially for marine and offshore construction, due to the durability and high capacity of the newly proposed pile, as well as its ability to overcome pile-soil interface problems.

Comparison of all Three Methods Used to Determine Ultimate Pile Capacities

Figure 12 presents a comparison of the ultimate capacities of all the piles investigated, as determined by the three methods used in this study. The ultimate capacities according to the Decourt method (1999) are slightly higher than those according to the other methods, due to the higher bearing capacity values and the large settlement at Q_{ult}. The modified Chin (1970) and Brinch Hansen (1963) methods yield similar results, except in the case of the sand-coated GFRP

pile S2000, where the total ultimate capacity determined by the Brinch Hansen method was a little higher than that determined by the modified Chin method. According to all three methods, the sand-coated pile S1500 had the highest ultimate capacity, and the control steel pile had the lowest ultimate capacity. The Brinch Hansen and Decourt methods found that the sand-coated piles S1500 and S2000 had the optimum ultimate pile capacities, whereas according to the modified Chin method the sand-coated piles S1500 and S1000 had the optimum ultimate pile capacities. All three methods showed that the ultimate pile capacity decreased when the sand coating density exceeded 2000 g/m^2, as was the case for the sand-coated GFRP pile S2500.

The proposed sand coated pile is not recommended to be used as a large-diameter hollow section pile. For medium diameter pile applications, the FRP pile needs to be checked to have enough capacity to prevent material and stability failure. If needed, the FRP pile can be filled with concrete to resist the expected loading.

The scaling effect in this study is minimal as the effect of the soil particle size is minimized as the ratio of the pile diameter to the mean particle size, D_{50}, of the foundation sand ranged from 102 to 122, and Bolton et al. (1999) showed that the soil particle size does not affect the results for ratios of the pile diameter to the mean particle size higher than 28. In addition, Ovesen (1979) showed that the particle size effects become significant only for pile circumference to D_{50} ratios between 20 and 40 for foundations on sand, Whereas, in this study, the ratio of the pile circumference to the mean particle size ranged from 310 to 380. Furthermore, the findings in this study for the ultimate friction capacity of the small-scale pile load tests are in line with the findings by Almallah et al. (2019) which provide the same trend of results for the interface friction angles between the GFRP specimens (sand coated/uncoated) and sand using a small interface shear box. This indicates that the scaling effect is not affecting the results trend in terms of the interlocking

between the soil particles and the sand coated GFRP specimens using the same sand coating density ratios in (g/m^2). Also, the scaling effect may not be significant if the only concern is the ultimate capacity, as the shaft capacity is often defined at a settlement given at a percentage of the shaft diameter, rather than at a fixed displacement (Sinnreich, 2011). Furthermore, in full-scale piles, the ultimate unit skin friction of piles in a given sand is practically independent of the pile diameter (Meyerhof, 1983).

Accordingly, in this study, the similarity law adopted for all conducted small-scale 1g laboratory pile tests was based on the pile length/pile diameter ratio (L/D) and using the same sand coating density ratios presented in Almallah et al. (2019). The reliability of the similarity law of small scale 1g testing system for FRP piles was justified by Sakr et al. (2005), and by Girlado et al. (2017).

Comparison between Experimental and Theoretical Calculated Ultimate Pile Capacities

The results of this experimental study found by using three different methods to estimate the ultimate pile capacities were compared with the theoretical design values calculated by using the interface friction angles determined by Almallah et al. (2019) for the interface of sand-coated GFRP piles in poorly graded sand as shown in Figure 13. The results of Almallah et al. (2019) follows the same pattern of results of the present study as the sand coated specimen S1500 indicated the optimum interface friction angle against dense sand. The ultimate bearing capacity was calculated theoretically for all piles as they have the same tip conditions based on Meyerhof (1976). The following equation was used to calculate the ultimate bearing capacity, Q_{ult}, of the pile:

$$Q_{ult} = A_s \, \bar{\sigma}_o \, k_s \tan(\delta) + \sigma_t N_q A_b \qquad (1)$$

Where A_s is the surface area of the shaft, $\bar{\sigma}_o$ is the average overburden stresses along the pile length, k_s is the lateral earth pressure coefficient for driven piles (taken as 5.04 for small-scale piles as per Sabry and Hanna 2009), $\tan(\delta)$ is the interface friction coefficient of the pile material with dense poorly graded sand as determined by Almallah et al. (2019) and presented in Figure 13 below, σ_t is the vertical stress at the pile tip, . N_q is the bearing capacity factor given by Meyerhof (1976), and A_b is the cross-sectional area of the pile tip.

Table 5 presents the calculated ultimate capacity design values for all the piles investigated in this study. Figure 14 shows that the experimentally determined ultimate capacities of all the piles are higher than the theoretical calculated ultimate capacities. For all of the experimental results, the total pile capacities differ from the theoretical results within a range of plus or minus 20%. It should be noted that, as in the case of the experimental results, the theoretically calculated pile capacities presented in Table 5 also indicate that of all the piles investigated, the sand-coated pile S1500 pile has the highest ultimate capacity.

Sand-Coated Pile Surfaces after Testing

To investigate the effects of pile driving and testing on the sand-coated surface of GFRP piles, and to examine how well the sand coating adheres to the pile surface, the weight of each pile per unit surface area was measured before and after testing. Before testing, the weight of the sand-coated GFRP piles per unit of surface area was 3864.7, 4134.4, 4820.6, 5585.2, and 6723.1 g/m^2 for piles S500, S1000, S1500, S2000, and S2500, respectively. After driving and testing, the weight of the composite piles per unit of surface area was 3778.4, 4052.6, 4750.6, 5329.7, and 6623.3 g/m^2, respectively. This comparison indicates that the loss of silica sand particles from the coating on the surface of GFRP piles during testing was insignificant. However, full-scale experiments are needed to check the bond between the coating substance and coating material under cyclic loading

conditions. To provide a visual comparison, Figure 15 presents photographs of the surfaces of two sand-coated GFRP piles before and after testing.

Test Repeatability

To ensure repeatability of the test results, a second sand-coated GFRP pile with a sand coating density of 1500 g/m^2 (S1500) was prepared and tested under axial loads. Figure 16 compares the results for the two S1500 piles, showing that the results are reliable and consistent for testing under the same conditions and that, of all the piles tested in this study, the sand-coated S1500 piles have the highest capacity. Table 6 summarizes the test repeatability results for the two S1500 sand-coated GFRP piles, as determined by the modified Chin method (1970).

CONCLUSIONS

This experimental study was conducted with the objective of enhancing the interface friction behaviour of GFRP piles in sand under axial loads, to provide an alternative to conventional pile construction materials. Five small-scale GFRP piles were coated in silica sand with different sand coating densities (500, 1000, 1500, 2000, and 2500 g/m^2). All five piles were instrumented and tested under axial loads in a soil box filled with dense poorly graded sand, by using a hydraulic jack connected to the top beam of a steel frame. The test results for the sand-coated GFRP piles were compared to the results for a control steel pile and two reference GFRP piles. The following conclusions can be drawn from the results of this study:

- Coating the surface of GFRP piles with silica sand enhanced the interface friction behaviour of the composite piles in sand under axial loads, as the interface friction was increased by interlocking between the soil particles and the sand-coated pile surface.

- In the pile load tests, of all the piles tested, the sand-coated GFRP pile S1500 with a sand coating density of 1500 g/m^2 had the highest ultimate pile capacity, as determined by the Brinch Hansen, modified Chin, and Decourt methods.
- As determined by the Brinch Hansen method, the total ultimate capacity of the S1500 pile was 23, and 31% greater than the ultimate capacities of the control GFRP-Rough and steel piles, respectively.
- A comparison of sand-coated GFRP piles before and after pile jacking (driving) and testing showed insignificant effects on the existing sand coating density confirming the reliability of the proposed technique to survive installation activities .
- The newly proposed mechanism of enhancing the interface friction behaviour of GFRP piles through sand coating was found to be effective under axial loads in sand. The results of this study are promising; however, future research on this new product is needed in different soil and loading conditions in order to refine the proposed concept. Furthermore, full-scale field tests are needed to verify the findings of this paper.

DATA AVAILABILITY

All data, models, and code generated or used during the study appear in the submitted article

ACKNOWLEDGMENTS

The authors express their gratitude to the student Ahmed Mahgoub for his extraordinary help and the students (Koosha Khorramian, Ahmed Moussa, Ali Iranikhah, and Georges Sarkis) and the technical staff (Jordan Maerz, Brian Kennedy, and Jesse Keane) of the Faculty of Engineering at Dalhousie University, Canada, for their endless support and help.

REFERENCES

[1] AASHTO. (2002). Standard specifications for highway bridges. Transportation officials.

[2] Abuel-Naga, H. M., & Shaia, H. A. (2014). Interface friction evolution of FRP tube confined concrete piles during the driving installation process. *Géotechnique Letters*, **4**(1), 52-56.

[3] Almallah, A., El Naggar, H., Sadeghian, P. (2018). *Direct shear tests of sandy soils interfaced with FRP sheets.* Paper presented at CSCE annual conference, Fredericton, Canada.

[4] Almallah, A., Sadeghian, P., El Naggar, H. (2020). Enhancing the interface friction between glass fiber-reinforced polymer sheets and sandy soils through sand coating, *Geomechanics and Geoengineering*, 15 (3), 186-202, https://doi.org/10.1080/17486025.2019.1635714

[5] Ashford, S. A., & Jakrapiyanun, W. (2001). Drivability of glass FRP composite piling. *Journal of Composites for Construction*, **5**(1), 58-60.

[6] ASTM A269/A269M-15a, Standard Specification for Seamless and Welded Austenitic Stainless-Steel Tubing for General Service.

[7] ASTM C136. (2014). Standard test method for sieve analysis of fine and coarse aggregates.

[8] ASTM D1143/D1143M. (2007). Standard Test Methods for Deep Foundations Under Static Axial Compressive Load.

[9] ASTM D2487. (2011). Standard practice for classification of soils for engineering purposes (unified soil classification system).

[10] ASTM D698. (2012). Standard test methods for laboratory compaction characteristics of soil using standard effort.

[11] Bryden, P., El Naggar, H., Valsangkar, A. (2014). Soil-structure interaction of very flexible pipes: centrifuge and numerical investigations. *International Journal of Geomechanics*, **15**(6), 04014091.

[12] Chin, F. K. (1970). Estimation of the ultimate load of piles from tests not carried to failure. In *Proc. 2nd Southeast Asian Conference on Soil Engineering,* Singapore.

[13] El Sharnouby, M. M., & El Naggar, M. H. (2018). Numerical Investigation of Axial Monotonic Performance of Reinforced Helical Pulldown Micropiles. *International Journal of Geomechanics*, **18**(10), 04018116.

[14] Fang, T., & Huang, M. (2019). Deformation and Load-Bearing Characteristics of Step-Tapered Piles in Clay under Lateral Load. *International Journal of Geomechanics*, **19**(6), 04019053.

[15] Frost, J. D., & Han, J. (1999). Behavior of interfaces between fiber-reinforced polymers and sands. *J Geotechnical and Geoenvironmental Eng*, **125**(8), 633-640.

[16] Giraldo Valez, J., & Rayhani, M. T. (2017). Axial and lateral load transfer of fibre-reinforced polymer (FRP) piles in soft clay. International Journal of Geotechnical Engineering, 11(2), 149-155.

[17] Guades, E. J., Aravinthan, T., and Islam, M. M. (2010). *An overview on the application of FRP composites in piling system.* Paper presented at the southern region engineering conference (SREC 2010), Toowoomba, Australia. 65-70.

[18] Guades, E. J., Aravinthan, T., Islam, M. M., & Manalo, A. (2012). A review on the driving performance of FRP composite piles. *Composite Structures*, **94**(6), 1932-1942.

[19] Iskander, M. G., & Hassan, M. (1998). State of the practice review in FRP composite piling. *J Composites for Construction*, **2**(3), 116-120.

[20] Mayerhof, G. G. (1976). Bearing capacity and settlement of pile foundations. *Journal of the Geotechnical Engineering Division.* American Society of Civil Engineers,102, 197-228.

[21] Meyerhof, G. G. (1983). Scale effects of ultimate pile capacity. Journal of Geotechnical Engineering, 109(6), 797-806.

[22] Nicola, A. D., & Randolph, M. F. (1999). Centrifuge modelling of pipe piles in sand under axial loads. *Géotechnique*, **49**(3), 295-318.

[23] Pei, H., Yin, J., Zhu, H., Hong, C. (2012). Performance monitoring of a glass fiber-reinforced polymer bar soil nail during laboratory pullout test using FBG sensing technology. *International Journal of Geomechanics*, **13**(4), 467-472.

[24] Sabry, M., & Hanna, A. (2009). Earth pressure acting on single driven piles in sand. Proceedings of the 17th International Conference on Soil Mechanics and Geotechnical Engineering, doi:10.3233/978-1-60750-031-5-125.

[25] Sakr, M., Naggar, M. H. E., & Nehdi, M. (2004). Novel toe driving for thin-walled piles and performance of fiberglass-reinforced polymer (FRP) pile segments. *Canadian geotechnical journal*, **41**(2), 313-325.

[26] Sakr, M., El Naggar, M. H., Nehdi, M. (2005). Interface characteristics and laboratory constructability tests of novel fiber-reinforced polymer/concrete piles. *J Composites for Construction*, **9**(3), 274-283.

[27] Sinnreich, J. (2011). The scaling effect of bored pile radius on unit shear capacity. *International Journal of Geotechnical Engineering*, *5*(4), 463-467.

[28] Soltannia, B., & Sameoto, D. (2014). Strong, reversible underwater adhesion via gecko-inspired hydrophobic fibers. *ACS applied materials & interfaces*, **6(**24), 21995-22003.

[29] Spiro, B. R., & Pais, M.A. (2002). Dynamic pile evaluation and pile load test results – test Piles TP#1, TP#2, and TP#3 at Spit Area, Pembroke Avenue Bridge Replacement, GSI Project, Hampton, VA, 1–2.

[30] Toufigh, V., Desai, C. S., Saadatmanesh, H., Toufigh, V., Ahmari, S., Kabiri, E. (2013). Constitutive modeling and testing of interface between backfill soil and fiber-reinforced polymer. *International Journal of Geomechanics*, **14(**3), 04014009.

[31] Toufigh, V., Ouria, A., Desai, C. S., Javid, N., Toufigh, V., Saadatmanesh, H. (2015). Interface behavior between carbon-fiber polymer and sand. *J Testing and Evaluation*, **44**(1), 385-390.

[32] Toufigh, V., Masoud Shirkhorshidi, S., Hosseinali, M. (2016). Experimental investigation and constitutive modeling of polymer concrete and sand interface. *International Journal of Geomechanics*, **17**(1), 04016043.

[33] Vineetha, V. J., & Ganesan, K. (2014). Interface Friction between Glass Fibre Reinforced Polymer and Gravel Soil. *In Advanced Materials Research*, 984, 707-710.

[34] Vipulanandan, C., D. Wong, M. Ochoa, and M. W. O'Neill. (1989). Modelling of displacement piles in sand using a pressure chamber. In *Foundation engineering: Current principles and practices*, ASCE, 526-541.

[35] Yang, J., Tham, L. G., Lee, P. K. K., Chan, S. T., Yu, F. (2006). Behaviour of jacked and driven piles in sandy soil. *Géotechnique*, **56**(4), 245-259.

[36] Zobel, H. et al. (2005). Kompozyty polimerowe w mostownistwie. *Materialy Budowlane*.

Table 1: Test Matrix for Pile Load Test

Group #	Specimen ID	Surface density of sand coating (g/m^2)	Pile outer diameter D (mm)	L/D	Description
1	Steel	0	50	15.2	Steel control
2	GFRP-Smooth	0	53	14.9	GFRP control
3	GFRP-Rough	0	54	14.1	GFRP control
4	GFRP-500	500	57	13.8	Sand-coated
5	GFRP-1000	1000	56	13.6	Sand-coated
6	GFRP-1500	1500	59	12.9	Sand-coated
7	GFRP-2000	2000	58	13.1	Sand-coated
8	GFRP-2500	2500	61	12.5	Sand-coated

Table 2 Ultimate Pile Capacities according to Brinch Hansen (1963)

Pile type	Ultimate capacity Q_{ult} (kN)	Settlement at Q_{ult} (mm)	Ultimate friction capacity Q_s (kN)	Ultimate bearing capacity Q_b (kN)	Sand relative density Dr%
Steel	10.7	19.7	2.7	8	74
GFRP-Smooth	11.5	15.8	2.9	8.6	75
GFRP-Rough	11.9	16.5	3.2	8.7	72
S500	13.1	14	4	9.1	77
S1000	13.4	17.7	4.4	9	74
S1500	15.5	24.6	6.7	8.8	76
S2000	14.1	19.7	5.3	8.8	74
S2500	12.1	12.4	3.9	8.2	73

Note: S stands for a sand-coated GFRP pile with the corresponding sand coating density

Table 3 Ultimate Pile Capacities according to the Modified Chin Method (1970)

Pile type	Ultimate capacity Q_{ult} (kN)	Settlement at Q_{ult} (mm)	Ultimate friction capacity Q_s (kN)	Ultimate bearing capacity Q_b (kN)	Sand relative density Dr%
Steel	10.9	7.1	2.8	8.1	74
GFRP-Smooth	11.4	15.5	2.8	8.6	75
GFRP-Rough	11.9	16.9	3.2	8.7	72
S500	13.1	14.9	4	9.1	77
S1000	13.4	18.2	4.5	8.9	74
S1500	15.3	22.1	6.7	8.6	76
S2000	13.2	16.1	5.2	8	74
S2500	12	12.8	3.9	8.1	73

Note: S stands for a sand-coated GFRP pile with the corresponding sand coating density

Table 4 Ultimate Pile Capacities according to the Decourt Method (1999)

Pile type	Ultimate capacity Q_{ult} (kN)	Settlement at Q_{ult} (mm)	Ultimate friction capacity Q_s (kN)	Ultimate bearing capacity Q_b (kN)	Sand relative density Dr%
Steel	11.8	19.6	2.7	9.1	74
GFRP-Smooth	12.1	25.1	2.8	9.3	75
GFRP-Rough	12.5	27.2	2.9	9.5	72
S500	14.1	27.1	4	10.1	77
S1000	14.2	28.3	4.6	9.6	74
S1500	15.5	27.6	6.7	8.8	76
S2000	14.4	29.2	5	9.4	74
S2500	13	25.6	4.3	8.7	73

Note: S stands for a sand-coated GFRP pile with the corresponding sand coating density

Table 5 Theoretical Calculated Ultimate Pile Capacities

Pile type	Ultimate capacity Q_{ult} (kN)	Ultimate friction capacity Q_s (kN)	Ultimate bearing capacity Q_b (kN)
Steel	10.6	2	8.6
GFRP-Smooth	11.3	2.7	8.6
GFRP-Rough	11.6	3	8.6
S500	11.9	3.3	8.6
S1000	12	3.4	8.6
S1500	12.8	4.2	8.6
S2000	12	3.4	8.6
S2500	11.8	3.2	8.6

Note: S stands for a sand-coated GFRP pile with the corresponding sand coating density

Table 6 Test Repeatability Results for two S1500 Sand-Coated GFRP Piles

Pile type	Ultimate capacity Q_{ult} (kN)	Settlement at Q_{ult} (mm)	Ultimate friction capacity Q_s (kN)	Ultimate bearing capacity Q_b (kN)	Sand relative density Dr%
1 S1500	15.3	22.1	6.7	8.6	76
2 S1500	16.9	29	7.7	9.2	78

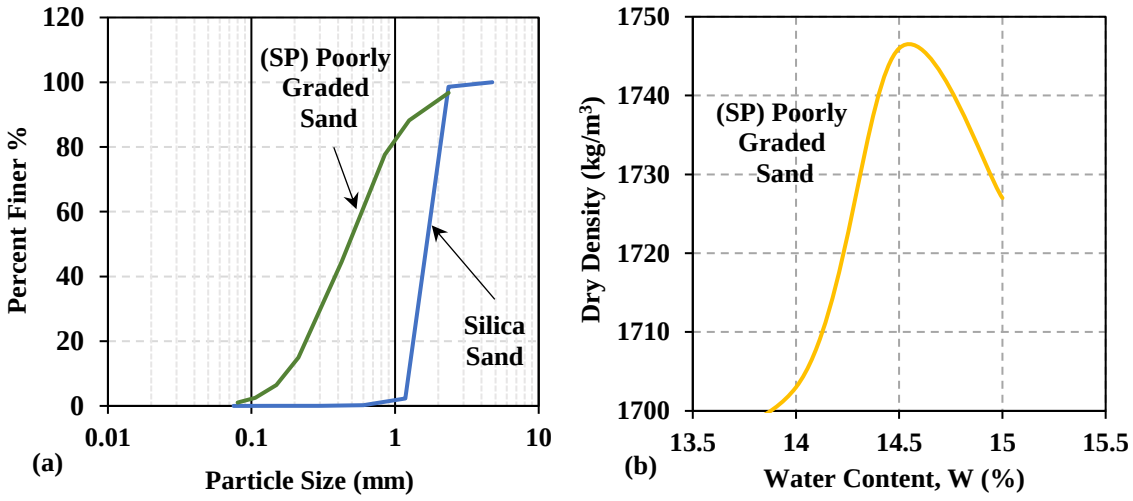

Figure 1 Soil properties: (a) gradation curves; and (b) maximum dry density vs. optimum water content

Figure 2 Fabrication of GFRP pile specimen: (a) material used for fabrication; (b) brushing the surface of the plastic pipe gently with epoxy resin and hardener; (c) brushing the first (90-degree hoop) layer of glass fabric with resin; (d) adding resin to the second and third (0-degree axial) layers of glass fabric; (e) adding resin to the last (90-degree hoop) layer of glass fabric; and (f) wax paper wrapped around the GFRP pile after completion of the pile layers

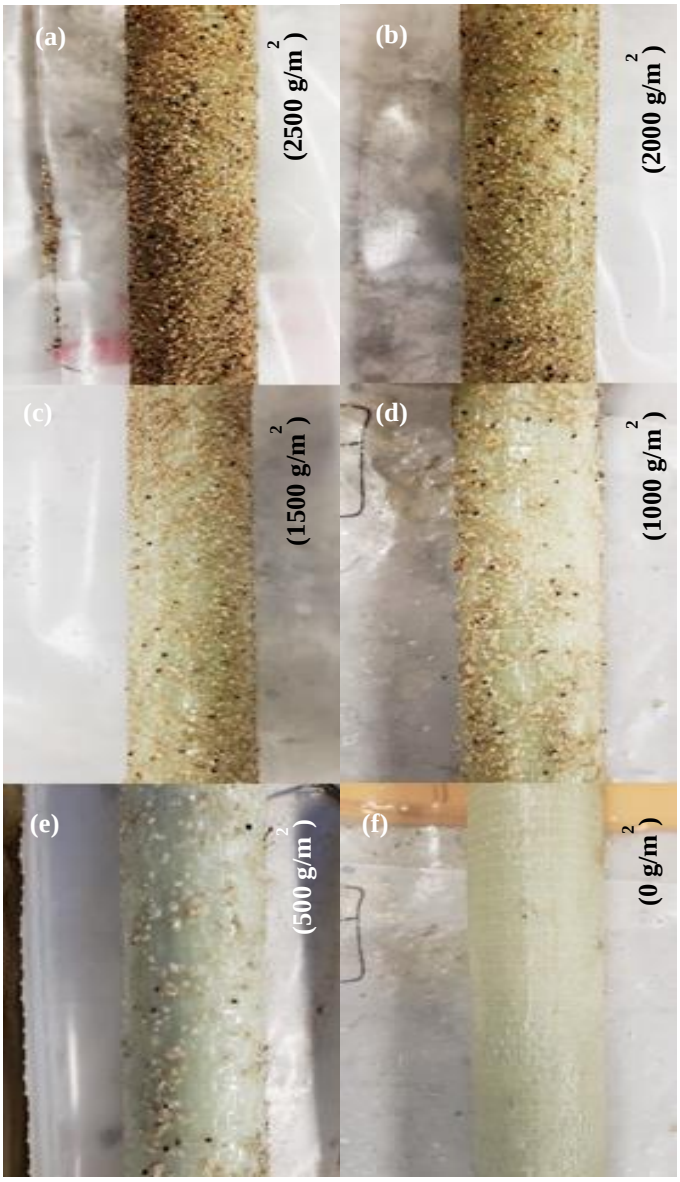

Figure 3 GFRP files with different sand coating densities: (a) GFRP-2500, (b) GFRP-2000, (c) GFRP-1500, (d) GFRP-1000, (e) GFRP-500, and (f) GFRP-Rough (GFRP-R)

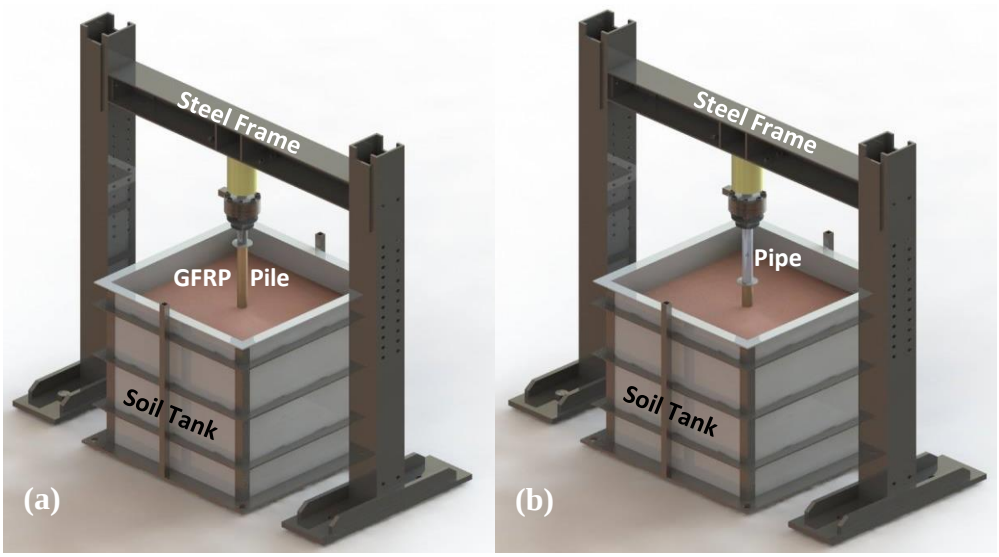

Figure 4 Schematic drawing of test setup and instrumentation: (a) first stage of jacking a GFRP pile; and (b) final stage of jacking a GFRP pile, using an aluminium extension pipe

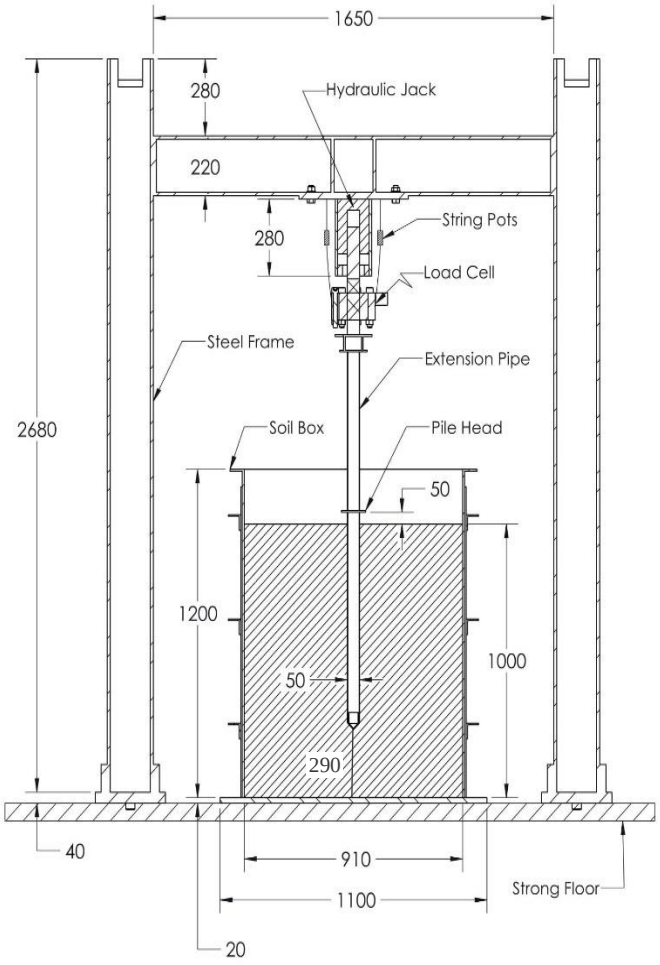

Figure 5 Detailed drawing showing pile load test setup after pile has been jacked-driven to the desired depth

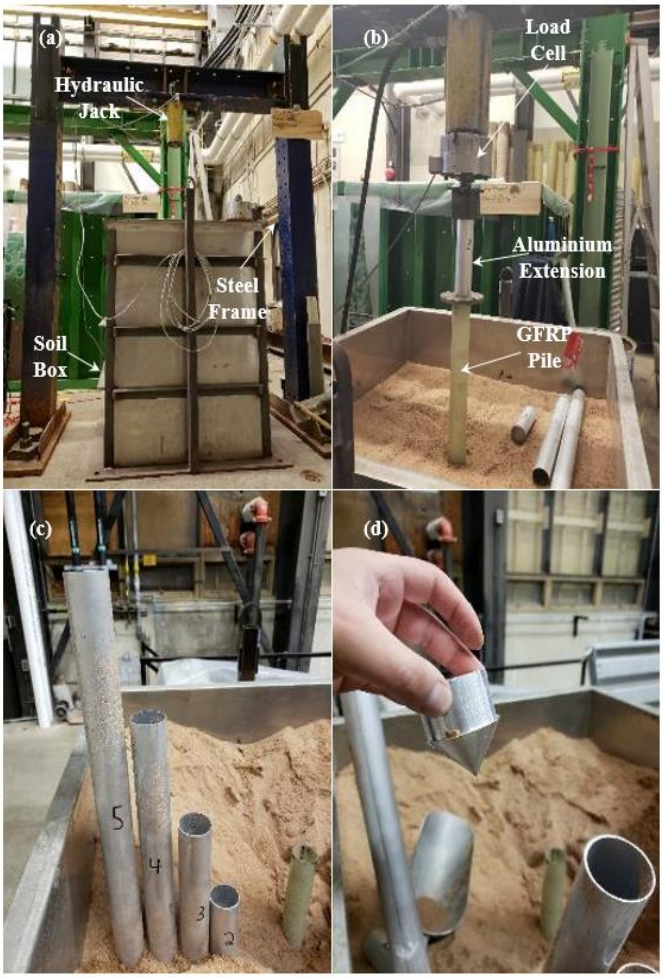

Figure 6 Test setup: (a) blue steel frame with soil tank and hydraulic jack; (b) the third stage of driving a GFRP pile, using the 280-mm aluminium extension pipe; (c) the four aluminium extension pipes, used for the different driving stages; and (d) cone-shaped pile toe

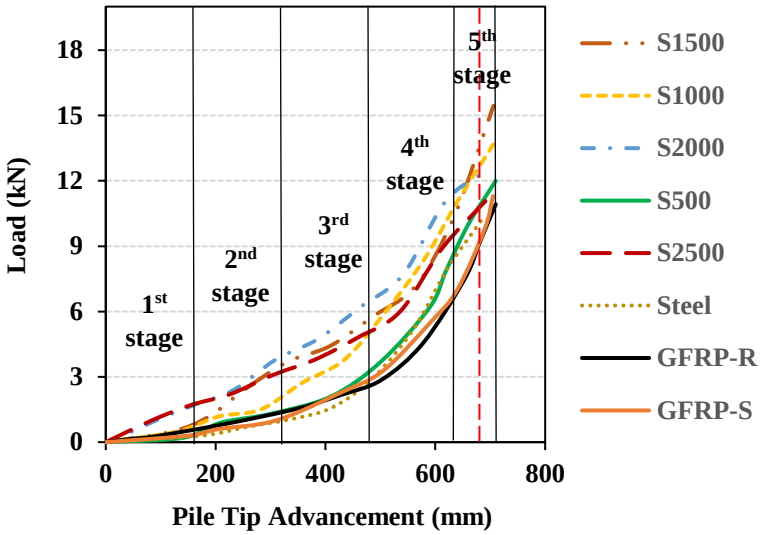

Figure 7 Jacking results for all eight piles

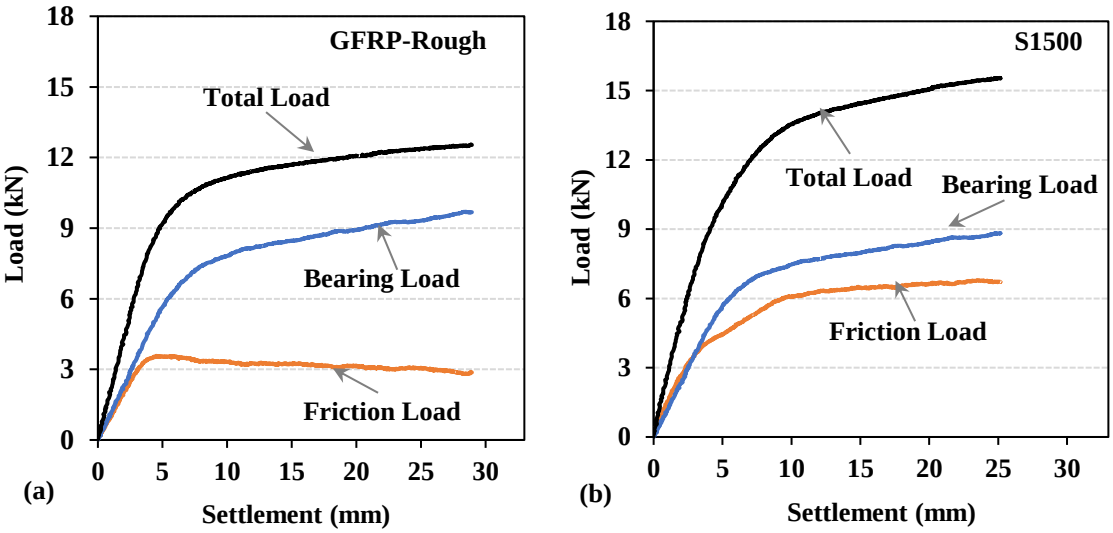

Figure 8 Pile load test results: (a) for the control pile GFRP-Rough; and (b) for the sand-coated GFRP-1500 pile (S1500)

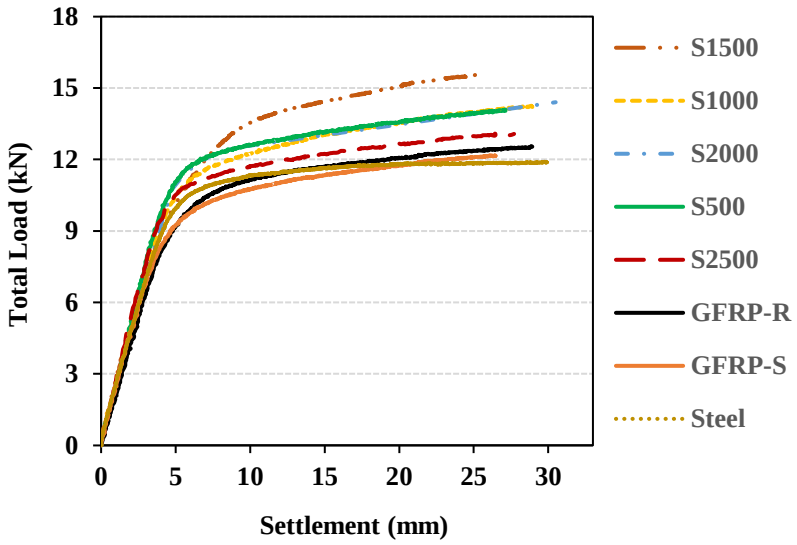

Figure 9 Pile load test results for all eight piles

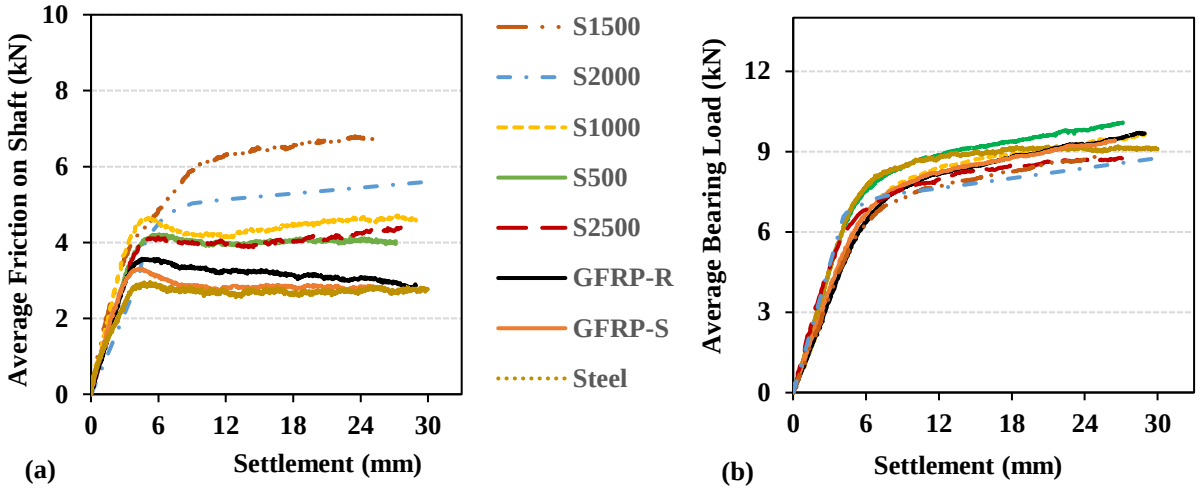

Figure 10 Pile load test results: (a) the average friction load along the pile shaft for each pile; and (b) the average bearing load at the pile tip for each pile

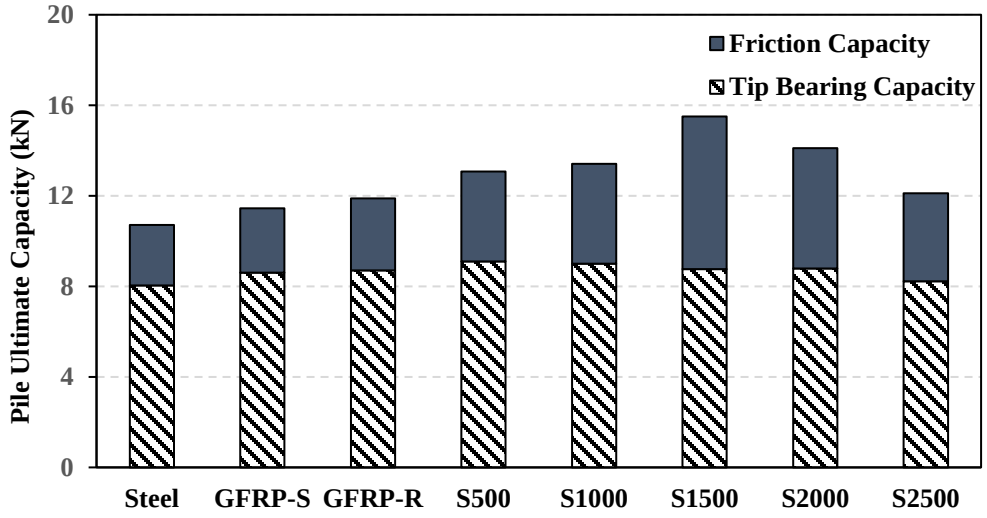

Figure 11: Ultimate pile capacities (Brinch Hansen method)

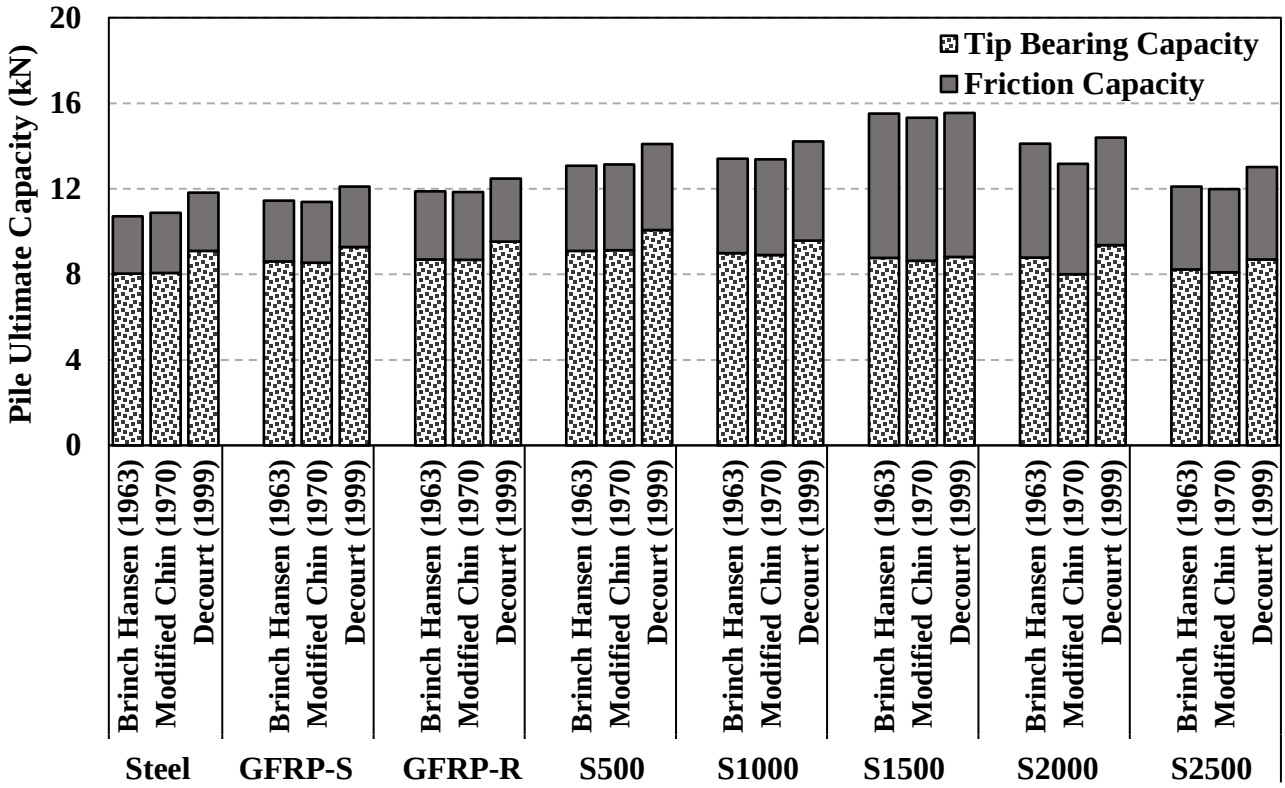

Figure 12 Comparison of ultimate pile capacities determined by all three methods used in this study

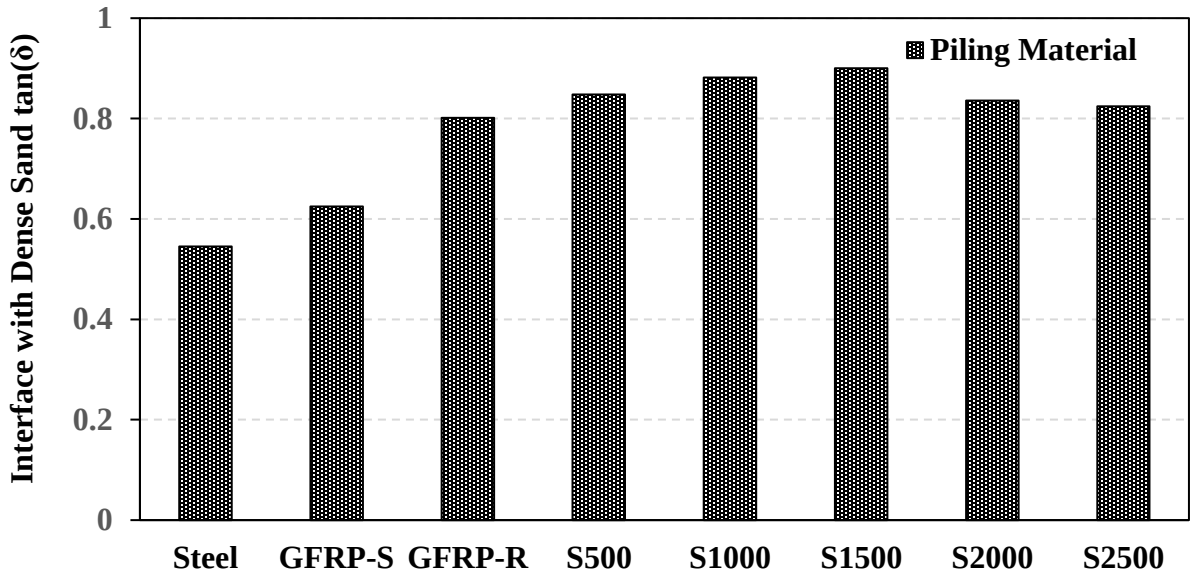

Figure 13 Interface friction angle between different piling materials and dense poorly graded sand (Almallah et al. 2019)

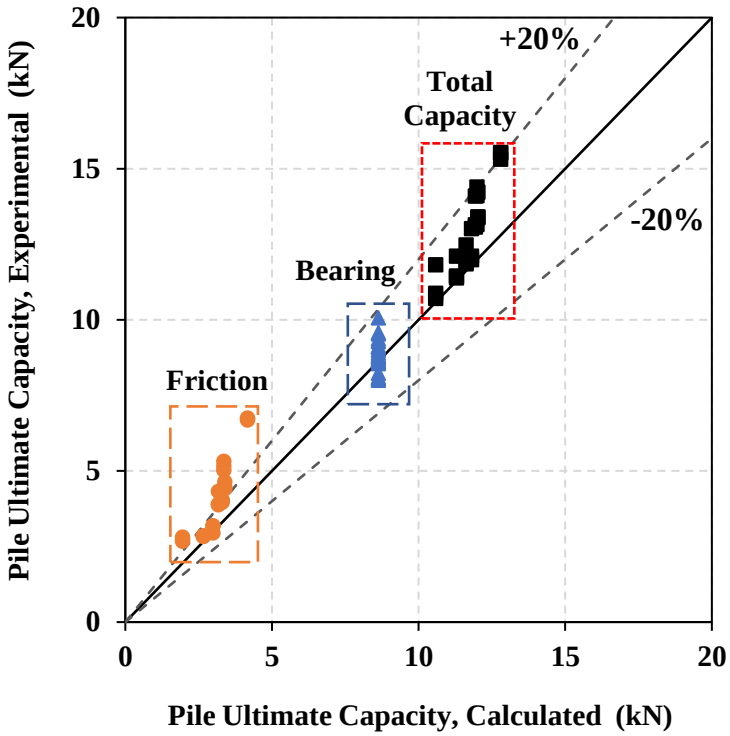

Figure 14 Comparison between experimentally determined and theoretically calculated ultimate pile capacities

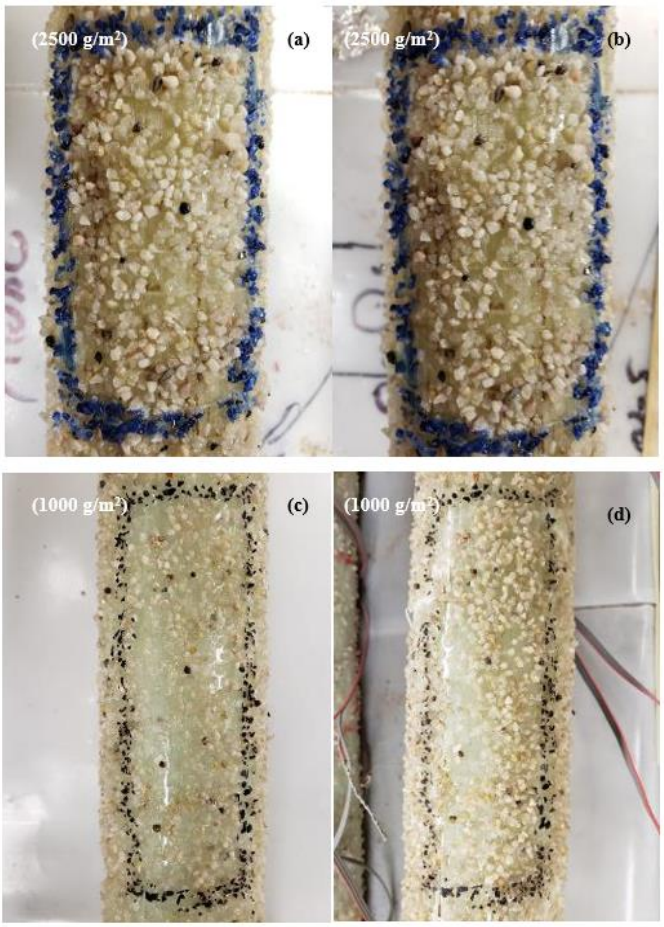

Figure 12 Sand-coated GFRP piles: (a) S2500 pile before testing; (b) S2500 pile after testing; (c) S1000 pile before testing; and (d) S1000 pile after testing

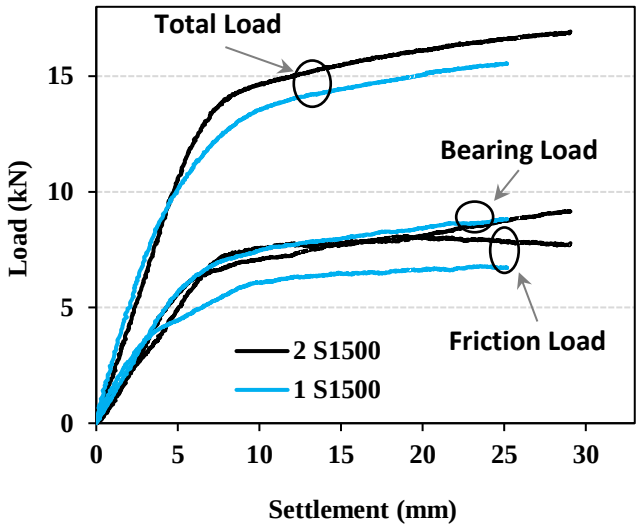

Figure 16 Pile load test results for two S1500 sand-coated GFRP piles